

Full length article



New reports on iron related proteins: Molecular characterization of two ferroportin genes in common carp (*Cyprinus carpio* L.) and its expression pattern

Teresa Kamińska-Gibas^a, Joanna Szczygieł^a, Annemiek Blasweiler^b, Łukasz Gajda^c, Ebru Yilmaz^d, Patrycja Jurecka^a, Ludmiła Kolek^a, Marek Ples^e, Ilgiz Irnazarow^{a,*}

^a Polish Academy of Sciences, Institute of Ichthyobiology and Aquaculture in Golysz, Zaborze, 43-520, Chybie, Poland

^b Aquaculture and Fisheries Group, Wageningen Institute of Animal Sciences, Wageningen University and Research, PO Box 338, 6700 AH, Wageningen, the Netherlands

^c Institute of Biology, Biotechnology and Environmental Protection, Faculty of Natural Sciences, University of Silesia in Katowice, Bankowa 9, 40-007, Katowice, Poland

^d Department of Aquaculture and Fisheries, Faculty of Agriculture, Aydın Adnan Menderes University, Aydın, Turkey

^e Department of Biomechatronics, Faculty of Biomedical Engineering, Silesian University of Technology, Roosevelta 40 Str., 41-800, Zabrze, Poland

ARTICLE INFO

Keywords:

Ferroportin
Iron metabolism
Hepcidin
Gene expression
Common carp

ABSTRACT

Iron uptake, transport, and storage require the involvement of several proteins, including ferroportin (*fpn*), the sole known iron efflux transporter. Due to its critical function *fpn* has been studied, particularly in humans. Here, we characterized the ferroportin gene in common carp (*Cyprinus carpio* L.) and performed RNA-seq analysis to evaluate its constitutive transcription levels across different tissues. Our results indicate that *C. carpio* possesses two functional *fpn*s with distinct expression patterns, highlighting the potential for functional divergence and expression differentiation among *fpn*s in this species.

1. Introduction

Iron is a crucial element for all living organisms, serving essential roles in biochemical processes such as ribonucleotide reduction, electron transfer, DNA replication, and transcription, as well as being critical to the formation of hemoglobin and myoglobin [1]. Iron's versatility results from its ability to form coordination complexes with organic ligands and its favorable redox potential, allowing interconversion between the ferrous (Fe(II)) and ferric (Fe(III)) states that facilitate biochemical reactions [2]. Although animals obtain iron primarily from food, they have not developed a pathway for excretion, necessitating a feedback mechanism to regulate intestinal iron absorption.

The balance between iron uptake, transport, and storage is regulated by a complex network of interacting proteins. Ferroportin (*fpn*, also known as SLC40A1) plays a crucial role as the sole known iron efflux transporter, moving iron from within cells to the bloodstream [3]. The amino acid sequence of *fpn* is highly conserved among vertebrates, and orthologs have been identified in worms and plants [4].

Ferroportin is a transmembrane protein, composed of two 6-transmembrane helix bundles (the N-lobe and C-lobe) joined by a long cytoplasmic loop, with its N- and C-termini located intracellularly [5,6]. Ferroportin expression is the highest in iron-rich tissues such as the liver, intestine, placenta, and macrophages, and its expression level is influenced by cellular hypoxia, iron concentration, and inflammation [7].

Another protein, hepcidin (*hep*), which is a small peptide produced in the liver, is closely linked to ferroportin activity [8]. Hepcidin serves as both an iron regulatory hormone and an antimicrobial peptide, regulating ferroportin through a negative feedback loop: hepcidin binding to *fpn* causes its ubiquitination, internalization, and degradation in lysosomes, reducing iron export and leading to a decrease in serum iron levels and hepcidin synthesis [9].

The majority of studies have focused on the interaction between human ferroportin and hepcidin, while little is known about this aspect in teleost fish. Given the role hepcidin plays in the immune system, there have been some studies conducted on this protein in fish. In fact, hepcidin has been identified and isolated in over 37 species of teleost [10].

Abbreviations: *fpn*, ferroportin; TM, transmembrane; *hep*, hepcidin; aa, amino acid; UTR, untranslated regions; IRP, iron regulatory protein; IRE, iron responsive elements; WGD, whole genome duplication; MS-222, Tricaine methanesulfonate; PBS, phosphate-buffered saline; BLAST, Basic Local Alignment Search Tool; RT, room temperature; cDNA, complementary DNA.

* Corresponding author.

E-mail address: ilgiz.irnazarow@golysz.pan.pl (I. Irnazarow).

<https://doi.org/10.1016/j.fsi.2023.109087>

Received 13 March 2023; Received in revised form 9 August 2023; Accepted 16 September 2023

Available online 28 September 2023

1050-4648/© 2023 The Author(s). Published by Elsevier Ltd. This is an open access article under the CC BY license (<http://creativecommons.org/licenses/by/4.0/>).

Detailed data on fish ferroportin is lacking, as it has only been characterized in a few species such as zebrafish [11], turbot [12], sea bass [13], and some others. Common carp hepcidin was identified a decade ago [14], but no research has been conducted on ferroportin so far. Common carp is an allotetraploid species, which undergone a whole-genome duplication event, resulting in the retention of two copies of its genome, known as subgenome A and subgenome B. The two subgenomes are highly similar, with an estimated nucleotide identity of 95–98% [15], still having some differences in gene content and expression patterns [16]. It is one of the earliest diverging teleost species and is believed to have diverged from the other teleosts approximately 8 million years ago [17]. As such, it occupies a key phylogenetic position and serves as an important reference point for understanding the evolution of other teleost species. These indicate the potential of the common carp genome as a valuable model for studying functional divergence and differentiation of expression in vertebrates.

In the present study, we aim to characterize ferroportin in common carp (*Cyprinus carpio* L.) and assess its constitutive transcription levels in various tissues.

2. Results

2.1. Ferroportin gene organization in common carp

As a result of the cloning approach and comparison of zebrafish ferroportin to carp genome, we identified two complete ferroportin variants. The syntenic relationship of these genes on chromosomes 42 and 47 suggests that they are orthologs of Danio's ferroportin gene placed on the 9 chromosome. This also corresponds to current genome annotation at A9 (for *fpn42*) and B9 (for *fpn47*) chromosomes. The full-length carp ferroportin gene assemblage has shown that both are composed of 8 exons and 7 introns, with the same size of exons but significantly varying in intron sizes and 5' and 3' untranslated regions (UTR) (Table 1).

Both coding DNA consists of an open reading frame of 1689 bp and translates into a 562 aa protein with predicted molecular weights of 61,8 kDa and 61,95 kDa for *fpn47* and *fpn42*, respectively. In addition, using an Iron Responsive Elements (IRE) database [18], a single IRE was predicted in the 5' UTR in both ferroportin genes (Supplementary Fig. 1).

2.2. Molecular model of carp ferroportin

Using the known human 3D structure, homology modelling was

Table 1

Comparison of the size of two putative ferroportin gene copies: *Fpn47* and *Fpn42*, located on chromosomes 47 and 42, respectively. The analysis is based on the *Common carp* genome available in GenBank under accession number GCA_905221575.1.

<i>C. carpio</i>	<i>Fpn47</i>	<i>Fpn42</i>
5'UTR	293	297
Exon 1	34	34
Intron 1	107	93
Exon 2	68	68
Intron 2	776	760
Exon 3	160	160
Intron 3	145	163
Exon 4	116	116
Intron 4	698	695
Exon 5	127	127
Intron 5	1180	1035
Exon 6	249	249
Intron 6	590	825
Exon 7	621	621
Intron 7	219	201
Exon 8	314	315
3'UTR	1780	1832

performed for *fpn47* and *fpn42* with a Phyre2 web server [19]. From a total of 562 residues, 429 (76%) were modelled at >90% confidence, and the remaining 133 residues were modelled *ab initio*. The secondary structure was predicted as twelve transmembrane helices arranged in two domains interconnected by a 78aa (*fpn47*) and 79aa (*fpn42*) cytoplasmic loop with both N- and C- terminal ends being placed intracellularly (Fig. 1). 99,8% and 100% of the residues lay in favorable and allowed regions of the Ramachandran plot for ferroportin 47 and 42, respectively.

2.3. Phylogenetic analysis and ferroportin comparison

Sequence comparison with other fish ferroportin proteins showed a high degree of conservation (Fig. 2). Functional domains like AP-2 adapter-binding motif for clathrin-dependent endocytosis and extracellular hepcidin-binding loop containing the Cys326 key residue have got high consensus with human ferroportin.

Phylogenetic analysis (Fig. 3) showed that Cypriniformes ferroportins are conserved and form a separate clade from those originated from other fish orders, i.e., Salmoniformes, Perciformes, and Tetraodontiformes. Afterward, Cypriniformes ferroportins were recovered as two well-separated subclades: Cobitidae and Cyprinidae. The latter was recovered as two clusters, albeit with low support (bootstrap support values below 75). The first cluster comprises Danioninae, Tincinae, Xenocypridinae, and Leuciscinae, while the second one comprises: Labeoninae and Cyprininae. Among the analyzed fish, more than two ferroportin variants were obtained for *Tor tambra* and *Cyprinus carpio*. Both species are known tetraploids [15]. While different UTR isoforms were found in *T. tambra*, resulting only in two non-identical proteins, four different coding sequence variants were retrieved in *C. carpio* for the analyzed specimen (i.e. double heterozygote in relation to ferroportin). In the latter species, the 'fnp47-like' isoform group was found, with high support, to be a sister to the group formed by 'fnp42-like isoforms' and *Carassius* spp. ferroportins. Moreover, the 'fnp47-like' isoform group was found to be a sister to *Carassius auratus* + *Carassius gibelio*, thus making the whole *C. carpio* ferroportin clade paraphyletic.

3. RNA-seq analysis: gene expression quantification

Heatmaps showing normalized read counts of the ferroportin gene in subgenome A and B of common carp for all seven tissues (liver, head kidney, intestine, gills, brain, muscle and gonads) separately (Fig. 4). The samples show the two different maturity and sex conditions that the tissues were sampled in; immature female, immature male, mature female and mature male. For each variant 3 fish was examined.

4. Discussion

In this study, we report the identification and characterization of ferroportin - the only known iron exporter - in common carp for the first time. Ferroportin is an ancient protein that exhibits high similarity among various vertebrates [6]. The comparison of putative common carp *fpn* genes with those of other fish and vertebrates revealed a high degree of conservation in their overall genomic architecture, amino acid sequence, and protein conformation. The total length of the coding sequences for ferroportin in common carp is 1689 bp, which is identical to that of *Carassius auratus* and zebrafish, other members of the *Cyprinidae* family [20] (see also Supplementary data Fig. S2). Both ferroportins in carp consist of 7 introns and 8 exons, a pattern also observed in most reported ferroportin genes in other fish species, including *Ictalurus punctatus*, *Scophthalmus maximus*, *Gadus morhua*, *Oryzias latipes*, and *Oncorhynchus mykiss* [21–24]. Although there were no differences in exon length between the two ferroportin genes in carp, the size of corresponding introns varied.

The IRE sequence was identified in the 5'-UTR region of *fpn42* and *fpn47*. Both isoforms have a 27-nucleotide sequence with CAGUGA

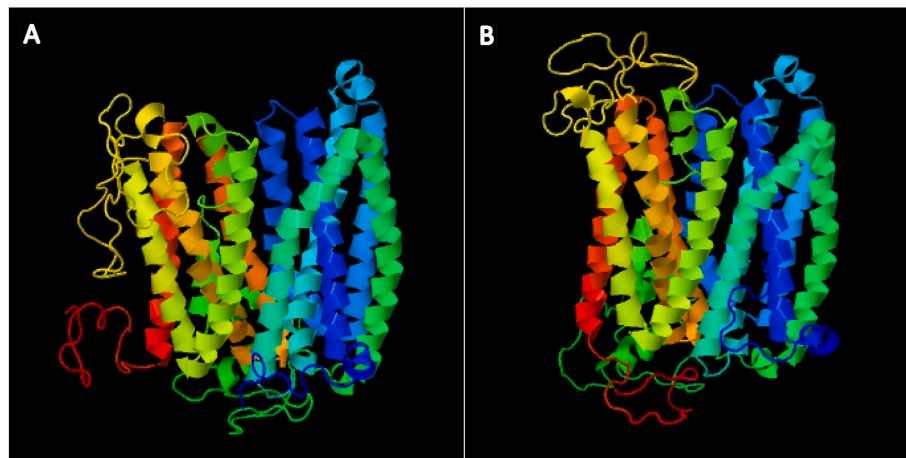


Fig. 1. Three-dimensional structure of common carp ferroportin 47 (A) and 42 (B) protein. Structure comprising 12 transmembrane helices with N-lobe (blue) and C-lobe (red) being placed intracellularly.

		20		40		60		80		100				
Cyprinus carpio 47	MEKAAS---	K	KPCFERYGEF	F	FKSAKFLIYL	GHALSTWGDR	MWNFAVAVFL	VELYGNLLLL	TAVYGLVVAG	SVLLLGAIIG	DWVDKNPRLK	VAQTSLVVQN	97	
Cyprinus carpio 42	DR..A---		.C.FC										97	
Danio rerio	DSP.....		RC.FR										97	
Labeo rohita	DS.....		SC.R										97	
Salmo salar	DN.G---		RCS.Q		T.P								97	
Takifugu rubripes	SSGP---		G.CVSI		RD.T								97	
Homo sapiens	TR.GDHN	RG.CG	SLADY	LT									100	
		120		140		160		180		200				
Cyprinus carpio 47	SAVILCGVLL	MAVFQFKVQL	TTLYNGWLLT	TCYIMVITIA	NIANLASTAM	SITIQRDVVV	VVAGDDRSKL	ADMNATVRII	DQLTNILAPM	LVGQIMAFGS			197	
Cyprinus carpio 42													197	
Danio rerio													197	
Labeo rohita													197	
Salmo salar													197	
Takifugu rubripes													197	
Homo sapiens													200	
		220		240		260		280		300				
Cyprinus carpio 47	HFIGCGFISG	WNLFSGMLEY	FLLWKVYQKT	PALAFKAGOK	DADDQELKHL	NVQKETGNSE	SPAEGSQ-LM	NETA-----	E	VKKNSTCCYO	MTEPIRTFKD		291	
Cyprinus carpio 42													291	
Danio rerio													291	
Labeo rohita													291	
Salmo salar													295	
Takifugu rubripes													279	
Homo sapiens													297	
		320		340		360		380		400				
Cyprinus carpio 47	GWVAYYNSI	FFAGMSLSFL	YMTVLGFD	CI	TTGAYY	TQGL	NGSVLS	LLMG	ASAISGICGT	VAFTWIRKCC	GLIRTFGIAG	VTQLSCLTLC	VASVFAPGSP	391
Cyprinus carpio 42														391
Danio rerio														391
Labeo rohita														391
Salmo salar														395
Takifugu rubripes														379
Homo sapiens														397
		420		440		460		480		500				
Cyprinus carpio 47	FDLSISPFD	EVLKHLFGDSG	SLRESPTLVP	TIEPKIQIN-	---AT--	VFE	KAPQVESYMS	VSLLFAGVIA	ARIGLWSFDL	TVTQLIQENV	IESERGIING		485	
Cyprinus carpio 42													485	
Danio rerio													485	
Labeo rohita													485	
Salmo salar													493	
Takifugu rubripes													473	
Homo sapiens													494	
		520		540		560		580		600				
Cyprinus carpio 47	VQNSMNYLLD	LLHFIMVILA	PNPEAFGLLV	IISVSFVAMG	HMMYFR	FAYK	SLRSRFLFC	SPEQKPD--P	NNPS-LPNSV				563	
Cyprinus carpio 42													563	
Danio rerio													563	
Labeo rohita													562	
Salmo salar													573	
Takifugu rubripes													551	
Homo sapiens													571	

Fig. 2. Alignment of ferroportin sequences. The human (*Homo sapiens*), Japanese pufferfish (*Takifugu rubripes*), Atlantic salmon (*Salmo salar*), rohu (*Labeo rohita*) and zebrafish (*Danio rerio*) sequences were aligned with both carp ferroportin sequences to demonstrate the conserved features and domains. Red frame – AP-2 adapter-binding motif for clathrin-dependent endocytosis, green frame – extracellular hepcidin-binding loop, blue arrow – key residue Cys326.

apical loop sequence for *fpn42* and CAGUGC for *fpn47*, indicating that they can bind to the iron regulatory protein (IRP) and are regulated by a translational control mechanism through the IRE-IRP system [6,25]. We compared the amino acid sequences of the common carp *fpn*s with those of other fish and human ferroportins. Both carp ferroportin genes contain all important functional domains, including the AP-2

adapter-binding motif for clathrin-dependent endocytosis, cytoplasmic loop responsible for hepcidin-dependent ubiquitination, and extracellular hepcidin-binding loop with a strictly conserved residue - Cys326. Interestingly, in some species (cartilaginous fish) where two ferroportin genes have been found, only one of them has the conserved Cys326 residue [6]. Therefore, the presence of Cys326 in both carp ferroportin

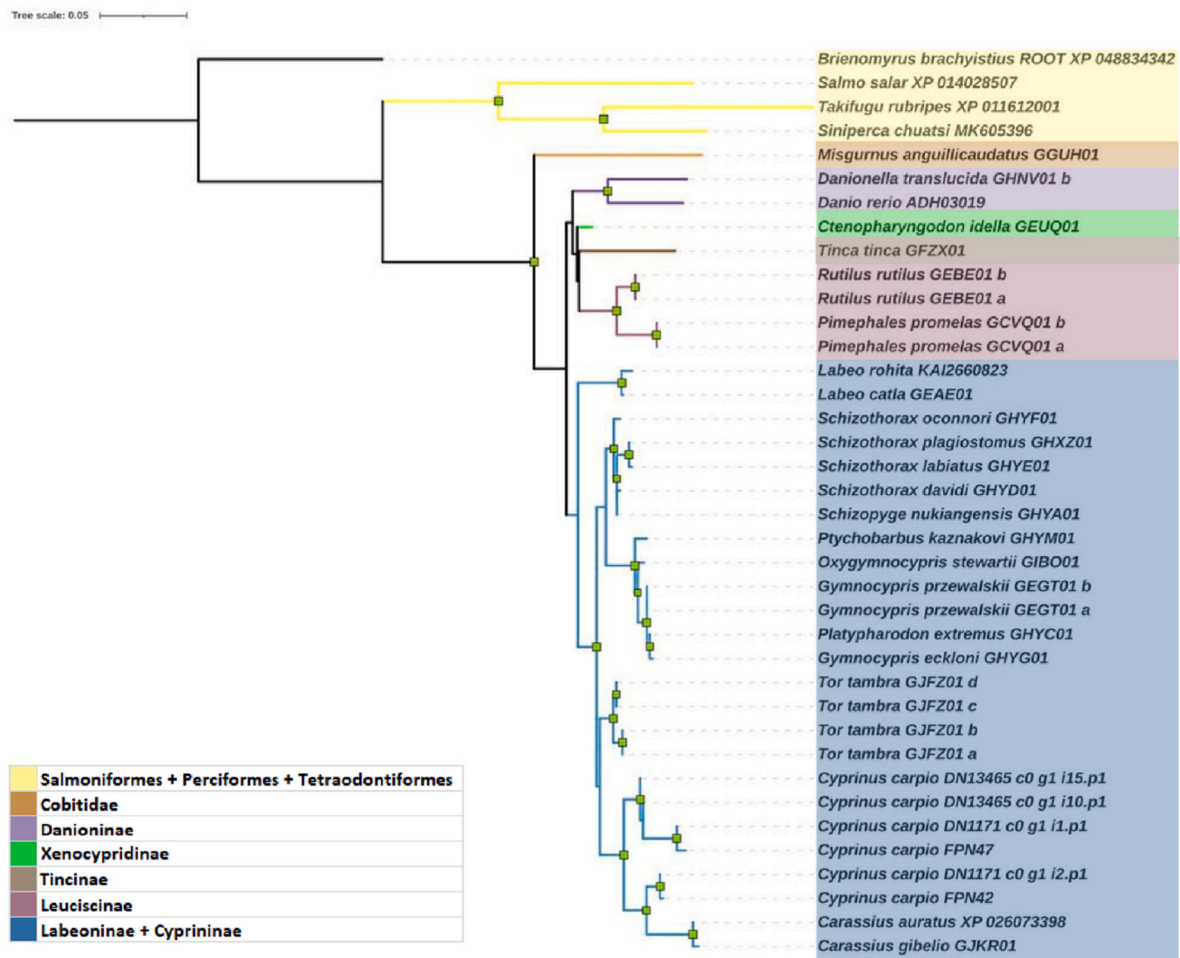


Fig. 3. Maximum likelihood tree resulting from the analysis of the putative ferroportin proteins in fish. Green squares denote branches with both SH-aLRT and UFBoot values of 75 or greater at the respective nodes. Sequences used in analysis were retrieved and generated mostly from transcriptomic data. A particular emphasis was given to Cypriniformes ferroportins. The tree was rooted at *Briomyrus brachyistius* (XP_048834342). The amino acid sequence alignment used to construct the presented tree and the sequence sources are included in Supplementary data (Fig. S2 and Table S1).

isoforms may indicate the functional activity of each isoform.

We used three-dimensional molecular modelling based on human ortholog model to study the common carp ferroportin. Our results revealed that it has 12 transmembrane domains (TM) with both N- and C-termini on the cytosolic side. Like humans, carp ferroportin also has a long cytoplasmic loop between TM6 and TM7, which divides it into two halves. The high similarity in amino acid sequence (76%) and protein conformation indicates that the mechanism of action of ferroportin in carp should be similar to that described for humans [26].

The separation of Cypriniformes ferroportins from those of other fish, as revealed by our phylogenetic analysis, is consistent with the results of a previous study by Neves et al. [13], in which the ferroportin sequence of *Danio rerio*, a member of the Cypriniformes order, was found to be distinct from homologous sequences in non-Cypriniformes fish. Furthermore, our ferroportin tree topology strongly supports the existing phylogenetic hypotheses related to Cypriniformes [27,28].

However, we did observe a high-support clade containing ferroportins from *Cyprinus carpio* and *Carassius* spp. (including *C. auratus*) that was found to be paraphyletic. This result can be attributed to the close relationship between the common carp and *Carassius* spp. [29], likely due to their shared ancestry within the *Barbinae* lineage [15].

Although we identified a double heterozygous specimen with four slightly different isoforms of ferroportin, genomic data only allowed us to predict two variants, one for each locus at chromosome A9 and B9 [30]. This may be due to the reference genome being generated from a

homozygous double-haploid clonal line [17], which could explain the “missing” isoforms observed in our RNA-seq results. Nevertheless, the common carp genome is an excellent model for studying functional divergence and expression differentiation in vertebrates, as the most recent whole genome duplication event occurred only 12 million years ago. Unlike other vertebrates, carp diploidization process was not that rapid and most ancestral genes remain duplicated, resulting in a high degree of gene retention and slow gene loss. However, expression divergence and functional differentiation were observed, as approximately half of duplicated gene pairs showed no strong correlation in expression [31].

Our RNA-seq analysis of seven different tissues from adult and juvenile fish, both male and female, revealed expression divergence between duplicated ferroportin genes. The count read charts showed three general groups: 1) high read counts with minor differences in expression between subgenomes in the liver and intestine, 2) higher expression of subgenome B ferroportin in the head kidney, brain, gills, and muscles, and 3) modest count reads for both subgenomes gonads. Tissue-specific expression of *fpn47* matched that of single *fpn* in other fish, with high expression levels in the liver, head kidney, intestine, gill, and brain, similar to that observed in sea bass [13]. Our findings suggests that both *fpn*s are actively expressing, but depending on the tissue they may differ in the degree of basal expression, showing a pattern that suggests possible divergence.

Similar observations were made by Braasch and colleagues [32] in

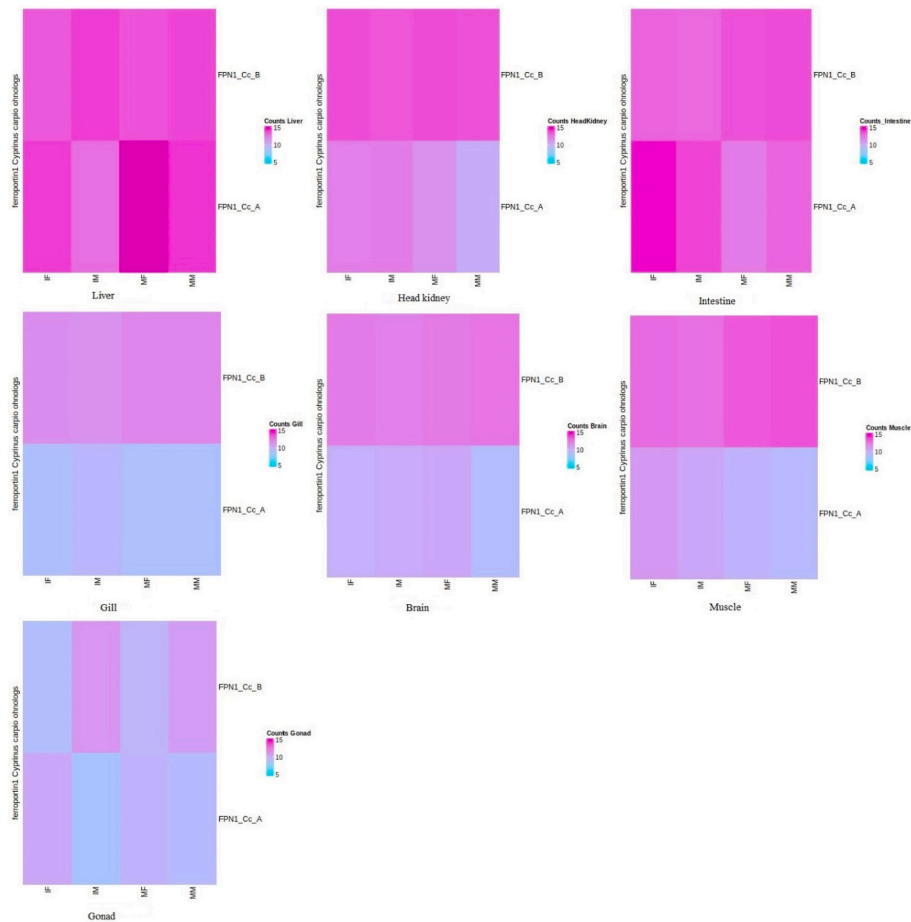


Fig. 4. RNA-seq normalized log₂ read counts for the two ferroportin genes of common carp in 7 tissues. FPN1_CcB indicates Ferroportin copy on chromosome 47. FPN1_CcA indicates Ferroportin copy on chromosome 42. Columns of the 7 heatmaps show 4 tissue sample conditions: IF (immature female), IM (immature male), MF (mature female), MM (mature male). Color scale shows the log₂ normalized counts.

zebrafish and eel, where each co-ortholog of the *prrx* gene exists in two forms (*prrx1a* and *prrx1b*), but with a clear predominance of *prrx1a* in expression. It is believed that the divergence of primary genomic sequence through base substitution, gain/loss of conserved noncoding elements (i.e., potential enhancers/promoters), and gain/loss of exons are key factors affecting the evolution of different expression of gene pairs [33]. In the case of *fpn* in common carp, we did not observe any changes in the number of exons between *fpn* copies, but we did observe differences in the genomic sequence. These differences may be due to the allotetraploid origin of common carp, or together with the divergence of the evolutionary branch in phylogenetic analysis, may indicate that *fpn42* is on different evolutionary path and may diverge into a gene with a new function.

The constitutive levels of ferroportin transcription can vary among different tissues in animals due to differences in iron storage and utilization [34]. Ferroportin plays a crucial role in iron homeostasis by exporting iron from cells. Tissues with high iron demand, such as the liver and bone marrow, have higher levels of ferroportin expression to support their iron needs, while tissues with lower iron requirements, such as skin and cartilage, have lower levels of ferroportin expression. Additionally, the levels of ferroportin expression can be regulated by various signaling pathways and transcription factors, which can vary among different tissues.

Based on our analysis of ferroportin expression and genetic variation in common carp, we have identified differences between duplicated ferroportin genes in terms of tissue-specific expression patterns and genomic sequence. Our findings supports thesis that the process of diploidization in the common carp genome has been relatively slow

[31], resulting in the retention of both genes copies and the development of functional differentiation and expression divergence. These results highlight the potential of the common carp genome as a valuable model for studying functional divergence and differentiation of expression in vertebrates.

Furthermore, our study underscores the importance of considering genetic variation and expression divergence when investigating the function and regulation of proteins which are crucial for homeostasis in animals.

Overall, our study contributes to a better understanding of the molecular mechanisms underlying iron homeostasis and gene expression regulation in vertebrates, with potential implications for the development of therapies targeting iron-related disorders.

5. Materials and methods

5.1. Fish sampling for tissue obtain

European common carp (*Cyprinus carpio* L.) strain R3xR8 which are the offspring of a cross between fish of Hungarian origin (R8 strain) and of Polish origin (R3 strain), with an average weight of 300 g was provided from the own resources of the Department of Ichthyobiology and Aquaculture, Polish Academy of Science, Golysz, Poland. Fish were reared at 20 °C in recirculating tank system and were fed dry food (Aller Aqua Polska Sp. z o. o., Poland) daily *ad libitum*. Before handling, fish were sedated using a MS-222 (Tricaine methanesulfonate, SigmaAldrich, Poland) solution of 150 mg/l in water or anesthetized with a dose of 500 mg/l. Animals were handled in accordance with good animal

practice by trained persons. All procedures were approved by the Local Ethics Committee and internal animal welfare authorities supervised the experiment.

5.2. Fish sampling for RNA-seq

European common carp (*Cyprinus carpio*) R3xR8 strain were used for RNA analysis. Eight-month and 2.5-year old fish were obtained from the Aquatic Research Facility of Carus (ARC), a part of Wageningen University & Research, The Netherlands. Fish were kept in a recirculatory closed water system at 24 °C with 12D:12L photoperiod and fed with pressed pellets for common carp (Skretting, Nutreco). Samples from 7 tissues were extracted and stored in RNA Later at -20 °C for further investigation.

5.3. Coding sequences identification and genomic organization of ferroportin genes

Coding sequences for ferroportin originating from *Danio rerio* and *Cyprinus carpio* genomes, available in the National Center for Biotechnology Information (<http://www.ncbi.nlm.nih.gov>) were used to perform Basic Local Alignment Searching (BLAST, CLC Main Workbench 7.0, Qiagen). Based on the alignment of identified putative coding sequences for ferroportin, the PCR primers were designed for further studies (Table 2).

Total RNA was isolated from the liver with the SV Total RNA Isolation System (Promega) and converted to cDNA with RevertAid RT Reverse Transcription Kit (Thermo Fisher Scientific). After PCR amplification (GenoPlast Biochemicals), obtained products were checked on 1.2% agarose gel and purified using a GenElute PCR Clean-up Kit (Sigma-Aldrich). Subsequently, the PCR products were cloned into p-GEM T-Easy Vector and then propagated in JM109 High-Efficiency Competent Cells (Promega) according to the manufacturer's instructions. Positive colonies were multiplied at 37 °C overnight in 5 ml of an LB medium containing 2.5 µl of ampicillin. Plasmid DNAs from at least 10 colonies were purified with GenoPlast Plasmid DNA extraction Kit (GenoPlast Biochemicals) and sent for sequencing (Nexbio, Lublin, Poland). Chromatograms were quality-analyzed, and then sequences were assembled. Coding DNA and genomic DNA were compared to identify intron/exon boundaries and flanking 5' and 3' regions. All analyses were performed using CLC Main Workbench 7.0 software (Qiagen).

5.4. Amino acid alignment and phylogenetic analysis

DNA sequences were translated to the corresponding peptide using VirtualRibosome 2.0 (<https://services.healthtech.dtu.dk/service.php?VirtualRibosome-2.0>). Amino acid sequences were aligned using MAFFT 7 [35] with automatic assignment of alignment strategy. A web server version of IQTREE [36] was used to find the best-fitting model of amino acid evolution and, subsequently, to construct a maximum likelihood tree. The tree was constructed using the JTT + G4 model as suggested by IQTREE, with 10,000 replications. Ultrafast bootstrap

Table 2

Oligonucleotide primers used to isolate the *Cyprinus carpio* ferroportin DNA sequences.

Gene	Primer	Sequence (5'-3')
Ferroportin	Fw1	AAAAACCTTGCTTTGGGCGAA
	Rv1	TAGCAGTGCTGGCCAGGTTA
	Fw2	CATCACCATTGCTAACATCGCT
	Rv2	GGTAGCAGCAACTGGTGTCT
	Fw3	AGGCTCCCAGTTGATGAATGA
	Rv3	CTCCAAACAGATGTTTCAAGACC
	Fw4	CCCTCGACGAGGTCTTGAAC
	Rv4	ACAGAGTTTGAAGTGAGGGATT

(UFBoots) support values were calculated using 1000 replicates with default settings. Subsequently, the SH-aLRT branch tests were used to evaluate tree branch supports. The tree was rooted to *Brienomyrus brachyistius* (XP_048834342) following the previous phylogenetic hypotheses [37].

5.5. Molecular 3D modelling of carp ferroportin

To generate the three-dimensional structure of carp ferroportin, the Phyre2 web server was exploited using an intensive analysis model. Twenty comparative models were generated with various confidence levels and % of identity. For further analysis, only the template with the highest degree of identity was selected to model the 3D structure c6wbvA – a human ferroportin with the confidence of 100% and 83% identity. The membrane topology of ferroportin was predicted with DeepTMHMM v1.0.12 (<https://dtu.biolib.com/DeepTMHMM>).

5.6. RNAseq –RNA isolation, gene expression quantification and structure analysis of common carp ferroportin

Total RNA was isolated from the head kidney using Quick-RNA Miniprep Kit (ZYMO Research). For all other tissue: liver, intestine, brain, muscle, gills and gonads, the miRNeasy Mini Kit (Qiagen) was used. The quantity of total RNA was assessed using Qubit 4 (Thermo Fisher Scientific). The Novogene UK Company LTD performed common carp transcriptome analysis using polyA RNA. Sequencing was carried out on an Illumina Novaseq 6000. Library preparation and cDNA synthesis was performed using NEBNext Ultra Directional RNA Library Prep Kit for Illumina. RNA reads were filtered and trimmed to remove adapters and low quality reads. Reads were aligned to the genome assembly of common carp *Cypcar_WagV4.0* available on ensembl (<http://www.ensembl.org>) with hisat2 v.4.8.2 [38]. Next RNA-seq reads were quantified with StringTie (v.2.1.5) [39]. Differential gene expression was analyzed using the bioinformatics package DESeq 2.0 (v1.26.0) by use of R (v.3.6.3) and Bioconductor (v.3.10.1) [40]. Additional analysis was performed based on the normalized counts obtained by the variance stabilizing transformation (VST) method of DESeq 2.0. The normalized counts were averaged into one condition based on the three replicates available. All heatmaps were created using the ComplexHeatmap [41] (v 2.2.0) package.

Financial disclosure statement

This research was supported by:

- National Science Centre, Poland grant number PRELUDIUM 2015/17/N/NZ6/03501
- European Union's Horizon 2020 Research and Innovation Programme under grant agreement No 817923 (AQUA-FAANG).

Institutional review board statement

This research was in compliance with Polish animal welfare regulations and approved by the Local Ethics Committee for Animal Experimentation in Katowice, Poland, license no May 2019 and the Animal Experiments Committee of Wageningen University and Research in accordance with the guidelines and regulations.

CRedit authorship contribution statement

Teresa Kamińska-Gibas: Conceptualization, Methodology, Investigation, Data curation, Preparation, Writing – review & editing, Acquisition. **Joanna Szczygiel:** Conceptualization, Methodology, Investigation, Data curation, Preparation, Acquisition. **Annemiek Blasweiler:** Methodology, Software, Preparation. **Łukasz Gajda:** Writing – original draft, Methodology, Preparation, Writing – review &

editing. **Ebru Yilmaz**: Investigation, Writing – review & editing. **Patrycja Jurecka**: Investigation. **Ludmila Kolek**: Investigation. **Marek Ples**: Investigation. **Ilgiz Irnazarow**: Conceptualization, Writing – review & editing, Supervision, Funding acquisition, Acquisition.

Declaration of competing interest

The authors declare no conflict of interest.

Data availability

Data will be made available on request.

Acknowledgements

We are grateful to Czesława Gaj-Chucher, Danuta Rajba-Nikiel, and Jolanta Krzemppek for their assistance in sampling. We also express our admiration for the professional skills of Michał Ingłot who took care of the fish. The authors also would like to thank the staff at the animal research facility “Carus” at Wageningen University for their assistance in the care of the animals and help with sampling.

Appendix A. Supplementary data

Supplementary data to this article can be found online at <https://doi.org/10.1016/j.fsi.2023.109087>.

References

- R.M. Graham, A.C.G. Chua, C.E. Herbison, J.K. Olynyk, D. Trinder, Liver iron transport, *World J. Gastroenterol.* 13 (35) (2007) 4725, <https://doi.org/10.3748/wjg.v13.i35.4725>, 473.
- G. Papanikolaou, K. Pantopoulos, Iron metabolism and toxicity, *Toxicol. Appl. Pharmacol.* 202 (2) (2005) 199–211, <https://doi.org/10.1016/j.taap.2004.06.021>.
- A. Donovan, C.N. Roy, N.C. Andrews, The ins and outs of iron homeostasis, *Physiol.* 21 (2) (2006) 115–123, <https://doi.org/10.1152/physiol.00052.2005>.
- T. Ganz, E. Nemeth, Iron homeostasis in host defence and inflammation, *Nat. Rev. Immunol.* 15 (2015) 500–510, <https://doi.org/10.1038/nri3863>.
- M.C. Bonaccorsi di Patti, F. Politicelli, G. Cece, A. Cutone, F. Felici, T. Persichini, G. Musci, A structural model of human ferroportin and of its iron binding site, *FEBS J.* 281 (12) (2014) 851–2860, <https://doi.org/10.1111/febs.12825>.
- E. Nemeth, T. Ganz, Heparin-ferroportin interaction controls systemic iron homeostasis, *Int. J. Mol. Sci.* 22 (2021) 6493, <https://doi.org/10.3390/ijms22126493>.
- A. Donovan, C.A. Lima, J.L. Pinkus, G.S. Pinkus, L.I. Zon, S. Robine, N.C. Andrews, The iron exporter ferroportin/Slc40a1 is essential for iron homeostasis, *Cell Metabol.* 1 (3) (2005) 191–200, <https://doi.org/10.1016/j.cmet.2005.01.003>.
- G. Nicolas, C. Chauvet, L. Viatte, J.L. Danan, X. Bigard, I. Devaux, C. Beaumont, A. Kahn, S. Vaulont, The gene encoding the iron regulatory peptide hepcidin is regulated by anemia, hypoxia, and inflammation, *J. Clin. Invest.* 110 (7) (2002) 1037–1044, <https://doi.org/10.1172/JCI15686>.
- I. De Domenico, D.M. Ward, C. Langelier, M.B. Vaughn, E. Nemeth, W.I. Sundquist, T. Ganz, G. Musci, J. Kaplan, The molecular mechanism of hepcidin-mediated ferroportin down-regulation, *Mol. Biol. Cell* 18 (2007) 2569–2578, <https://doi.org/10.1091/mbc.e07-01-0060>.
- J. Chen, W. Jiang, Y.-W. Xu, R.-Y. Chen, Q. Xu, Sequence analysis of hepcidin in barbel steed (*Hemibarbus labeo*): QSHLS motif confers hepcidin iron-regulatory activity but limits its antibacterial activity, *Dev. Comp. Immunol.* 114 (2021), <https://doi.org/10.1016/j.dci.2020.103845>.
- A. Donovan, A. Brownlie, Y. Zhou, J. Shepard, S.J. Pratt, J. Moynihan, B.H. Paw, A. Drejer, B. Barut, A. Zapata, T.C. Law, C. Brugnara, S.E. Lux, G.S. Pinkus, J. L. Pinkus, P.D. Kingsley, J. Palis, M.D. Fleming, N.C. Andrews, L. Zon, Positional cloning of zebrafish ferroportin1 identifies a conserved vertebrate iron exporter, *Nature* 403 (2000) 776–781, <https://doi.org/10.1038/35001596>.
- C.-G. Yang, S.-S. Liu, B. Sun, X.-L. Wang, N. Wang, S.-L. Chen, Iron-metabolic function and potential antibacterial role of hepcidin and its correlated genes (Ferroportin 1 and Transferrin Receptor) in Turbot (*Scophthalmus maximus*), *Fish Shellfish Immunol.* 34 (3) (2013) 744–755, <https://doi.org/10.1016/j.fsi.2012.11.049>, 3.
- J.V. Neves, M.F. Ramos, A.C. Moreira, T. Silva, M.S. Gomes, P.N.S. Rodrigues, Hamp1 but not Hamp2 regulates ferroportin in fish with two functionally distinct hepcidin types, *Sci. Rep.* 7 (2017), 14793, <https://doi.org/10.1038/s41598-017-14933-5>.
- H. Li, F. Zhang, H. Guo, Z. Zhu, J. Yuan, G. Yang, L. An, Molecular characterization of hepcidin gene in common carp (*Cyprinus carpio* L.) and its expression pattern responding to bacterial challenge, *Fish Shellfish Immunol.* 35 (3) (2013) 1030–1038, <https://doi.org/10.1016/j.fsi.2013.07.001>.
- P. Xu, J. Xu, G. Liu, L. Chen, Z. Zhou, W. Peng, Y. Jiang, Z. Zhao, Z. Jia, Y. Sun, Y. Wu, B. Chen, F. Pu, J. Feng, J. Luo, J. Chai, H. Zhang, H. Wang, C. Dong, W. Jiang, X. Sun, The allotetraploid origin and asymmetrical genome evolution of the common carp *Cyprinus carpio*, *Nat. Commun.* 10 (2019) 4625, <https://doi.org/10.1038/s41467-019-12644-1>.
- J. Luo, J. Chai, Y. Wen, M. Tao, G. Lin, X. Liu, L. Ren, Z. Chen, S. Wu, S. Li, Y. Wang, Q. Qin, S. Wang, Y. Gao, F. Huang, L. Wang, C. Ai, X. Wang, L. Li, C. Ye, H. Yang, M. Luo, J. Chen, H. Hu, L. Yuan, L. Zhong, J. Wang, J. Xu, Z. Du, Z.S. Ma, R.W. Murphy, A. Meyer, J. Gui, P. Xu, J. Ruan, Z.J. Chen, S. Liu, X. Lu, Y.P. Zhang, From asymmetrical to balanced genomic diversification during rediploidization: subgenomic evolution in allotetraploid fish, *Sci. Adv.* 6 (22) (2020) 7677, <https://doi.org/10.1126/sciadv.aaz7677>.
- P. Xu, X. Zhang, X. Wang, J. Li, G. Liu, Y. Kuang, J. Xu, X. Zhenh, L. Ren, G. Wang, Y. Zhang, L. Huo, Z. Zhao, D. Cao, C. Lu, C. Li, Y. Zhou, Z. Liu, Z. Fan, G. Shan, X. Li, S. Wu, L. Song, G. Hou, Z. Sun, Genome sequence and genetic diversity of the common carp, *Cyprinus carpio*, *Nat. Genet.* 46 (2014) 1212–1219, <https://doi.org/10.1038/ng.3098>.
- B. Wang, M.S. Thompson, K.M. Adkins, Characteristics of the iron-responsive element (IRE) stems in the untranslated regions of animal mRNAs, *Open Biochem. J.* 15 (2021) 26–37, <https://doi.org/10.2174/1874091X02115010026>.
- L. Kelley, S. Mezulis, C. Yates, M.W. Wass, M.J.E. Sternberg, The Phyre2 web portal for protein modeling, prediction and analysis, *Nat. Protoc.* 10 (2015) 845–858, <https://doi.org/10.1038/nprot.2015.053>.
- A. Rafiee, S. Fatemi, S. Jamili, S. Ajdari, F. Riazi-Rad, A. Memarnejadian, M. Alimohammadian, Cloning, expression and characterization of Zebra fish ferroportin in hek 293T cell line, *Iran. J. Public Health* 41 (1) (2012) 79–86.
- S. Liu, Y. Zhang, Z. Zhou, G. Waldbieser, F. Sun, J. Lu, J. Zhang, Y. Jiang, H. Zhang, X. Wang, K.V. Rajendran, L. Khoo, H. Kucuktas, E. Peatman, Z. Liu, Efficient assembly and annotation of the transcriptome of catfish by RNA-Seq analysis of a doubled haploid homozygote, *BMC Genom.* 13 (2012) 595, <https://doi.org/10.1186/1471-2164-13-595>.
- P. Pereira, A. Figueras, B. Novoa, A novel hepcidin-like in turbot (*Scophthalmus maximus* L.) highly expressed after pathogen challenge but not after iron overload, *Fish Shellfish Immunol.* 32 (2012) 879–889, <https://doi.org/10.1016/j.fsi.2012.02.016>.
- B. Star, A.J. Nederbragt, S. Jentoft, U. Grimholt, M. Malmstrøm, T.F. Gregers, T. B. Rounge, J. Paulsen, M.H. Solbakken, A. Sharma, O.F. Wetten, A. Lanzén, R. Winer, J. Knight, J.H. Vogel, B. Aken, O. Andersen, K. Lagesen, A. Tooming-Klunderud, R.B. Edvardsen, K.G. Tina, M. Espelund, C. Nepal, C. Prevti, B. O. Karlsén, T. Moum, M. Skage, P.R. Berg, T. Gjoen, H. Kuhl, J. Thorsen, K. Malde, R. Reinhardt, L. Du, S.D. Johansen, S. Searle, S. Lien, F. Nilsen, I. Jonassen, S. W. Omholt, N.C. Stenseth, K.S. Jakobsen, The genome sequence of Atlantic cod reveals a unique immune system, *Nature* 477 (7363) (2011) 207–210, <https://doi.org/10.1038/nature10342>.
- J. Pasquier, C. Cabau, T. Nguyen, E. Jouanno, D. Severac, I. Braasch, L. Journot, P. Pontarotti, C. Klopp, J.H. Postlethwait, Y. Guiguen, J. Bobe, Gene evolution and gene expression after whole genome duplication in fish: the PhyloFish database, *BMC Genom.* 17 (2016) 368, <https://doi.org/10.1186/s12864-016-2709-z>.
- P. Piccinelli, T. Samuelsson, Evolution of the iron-responsive element, *RNA* 13 (7) (2007) 952–966, <https://doi.org/10.1261/rna.464807>.
- C.B. Billesbølle, C.M. Azumaya, R.C. Kretsch, A.S. Powers, S. Gonen, S. Schneider, T. Arvedson, R.O. Dror, Y. Cheng, A. Manglik, Structure of hepcidin-bound ferroportin reveals iron homeostatic mechanisms, *Nature* 586 (2020) 807–811, <https://doi.org/10.1038/s41586-020-2668-z>.
- L. Yang, M. Arunachalam, T. Sado, B.A. Levin, A.S. Golubtsov, J. Freyhof, J.P. Friel, W.J. Chen, M.V. Hirt, R. Manickam, M.K. Agnew, A.M. Simons, K. Saitoh, M. Miya, R.L. Mayden, S. He, Molecular phylogeny of the cyprinid tribe Labeonini (Teleostei: Cypriniformes), *Mol. Phylogenet. Evol.* 65 (2) (2012) 362–379, <https://doi.org/10.1016/j.ympev.2012.06.007>.
- W. Tao, L. Yang, R.L. Mayden, S. He, Phylogenetic relationships of Cypriniformes and plasticity of pharyngeal teeth in the adaptive radiation of cyprinids, *Sci. China Life Sci.* 62 (4) (2019) 553–565, <https://doi.org/10.1007/s11427-019-9480-3>.
- O.V. Apalikova, A.V. Podlesnykh, A.D. Kuchklevskii, S. Gokhva, V.A. Brykov, Phylogenetic relationships of silver crucian carp *Carassius auratus gibelio*, *C. auratus cuvieri*, crucian carp *C. carassius*, and common carp *Cyprinus carpio* as inferred from mitochondrial DNA variation, *Genetika* 47 (3) (2011) 368–378.
- J.T. Li, Q. Wang, M.D. Huang Yang, Q.-S. Li, M.-S. Cui, Z.-J. Dong, H.-W. Wang, J.-H. Yu, C.-R. Yang, Y.-X. Wang, X.-Q. Sun, Y. Zhang, R. Zhao, Z.-Y. Jia, X.-Y. Wang, Parallel subgenomic structure and divergent expression evolution of allo-tetraploid common carp and goldfish, *Nat. Genet.* 53 (2021) 1493–1503, <https://doi.org/10.1038/s41588-021-00933-9>.
- J.-T. Li, G.-Y. Hou, X.-F. Kong, C.-Y. Li, J.-M. Zeng, H.-D. Li, G.-B. Xiao, X.-M. Li, X.-W. Sun, The fate of recent duplicated genes following a fourth-round whole genome duplication in a tetraploid fish, common carp (*Cyprinus carpio*), *Sci. Rep.* 5 (2015) 8199, <https://doi.org/10.1038/srep08199>.
- I. Braasch, Y. Guiguen, R. Loker, J.H. Letaw, A. Ferrara, J. Bobe, J.H. Postlethwait, Connectivity of vertebrate genomes: paired-related homeobox (Prrx) genes in spotted gar, basal teleosts, and tetrapods, *Comp. Biochem. Physiol. C Toxicol. Pharmacol.* 163 (2014) 24–36, <https://doi.org/10.1016/j.cbpc.2014.01.005>.
- Z. Chen, Y. Omori, S. Koren, T. Shirokiya, T. Kuroda, A. Miyamoto, H. Wada, A. Fujiyama, A. Toyoda, S. Zhang, T.G. Wolfsberg, K. Kawakami, A.M. Phillippy, J. C. Mullikin, S.M. Burgess, De novo assembly of the goldfish (*Carassius auratus*) genome and the evolution of genes after whole-genome duplication, *Sci. Adv.* 5 (6) (2019) 1–12, <https://doi.org/10.1126/sciadv.aav0547>.

- [34] E. Gammella, M. Correnti, G. Cairo, S. Recalcati, Iron availability in tissue microenvironment: the key role of ferroportin, *Int. J. Mol. Sci.* 22 (6) (2021) 2986, <https://doi.org/10.3390/ijms22062986>.
- [35] K. Katoh, J. Rozewicki, K.D. Yamada, MAFFT online service: multiple sequence alignment, interactive sequence choice and visualization, *Briefings Bioinf.* 20 (4) (2019) 1160–1166, <https://doi.org/10.1093/bib/bbx108>.
- [36] J. Trifinopoulos, L.-T. Nguyen, A. von Haeseler, Quang Minh, B. W-Iq-Tree, A fast online phylogenetic tool for maximum likelihood analysis, *Nucleic Acids Res.* 44 (1) (2016) 232–235, <https://doi.org/10.1093/nar/gkw256>.
- [37] R. Betancur-R, E.O. Wiley, G. Arratia, A. Acero, M. Miya, G. Lecointre, G. Orti, Phylogenetic classification of bony fishes, *BMC Evol. Biol.* 17 (2017) 162, <https://doi.org/10.1186/s12862-017-0958-3>.
- [38] D. Kim, J.M. Paggi, C. Park, C. Bennett, S.L. Salzberg, Graph-based genome alignment and genotyping with HISAT2 and HISAT-genotype, *Nat. Biotechnol.* 37 (8) (2019) 907–915, <https://doi.org/10.1038/s41587-019-0201-4>.
- [39] M. Pertea, D. Kim, G.M. Pertea, J.T. Leek, S.L. Salzberg, Transcript-level expression analysis of RNA-seq experiments with HISAT, StringTie and Ballgown, *Nat. Protoc.* 11 (9) (2016) 1650–1667, <https://doi.org/10.1038/nprot.2016.095>.
- [40] M.I. Love, W. Huber, S. Anders, Moderated estimation of fold change and dispersion for RNA-seq data with DESeq2, *Genome Biol.* 15 (12) (2014) 1–21, <https://doi.org/10.1186/s13059-014-0550-8>.
- [41] Z. Gu, R. Eils, M. Schlesner, Complex heatmaps reveal patterns and correlations in multidimensional genomic data, *Bioinformatics* 32 (18) (2016) 2847–2849, <https://doi.org/10.1093/bioinformatics/btw313>.